

TI Designs

High Dynamic-Range Headphone Driver Reference Design for Voltage-Output, Differential Audio DACs



TI Designs

TI Designs provide the foundation that you need including methodology, testing and design files to quickly evaluate and customize the system. TI Designs help you accelerate your time to market.

Design Resources

TIDA-00715	Tool Folder Containing Design Files
OPA2836	Product Folder
THS4521	Product Folder
OPA1632	Product Folder
TINA-TI™	Tools Folder



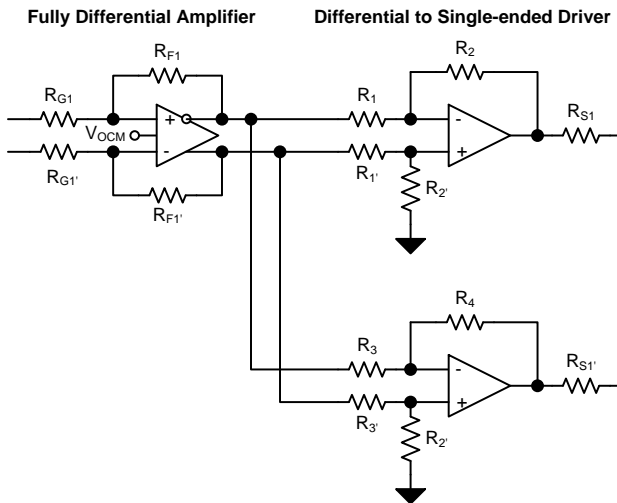
[ASK Our E2E Experts](#)
[WEBENCH® Calculator Tools](#)

Design Features

- Features a High-Performance, Low-Distortion, Audio-Amplifier Signal Chain
- Explores Various Trade-offs to Extract Optimum Performance Based on System Needs
- Includes Low Distortion, Fully-Differential Stage to Amplify Signal From Voltage Out Audio DAC Such as PCM1791A
- Features a Differential to Single-Ended 2nd Stage Amplifier Utilizing Load Sharing to Drive Headphone Load
- Can be Extended to Current Output Audio DACs Such as PCM1792A by Configuring FDA as a Transimpedance Amplifier

Featured Applications

- Headphone Driver for Voltage-Output Audio DAC



An IMPORTANT NOTICE at the end of this TI reference design addresses authorized use, intellectual property matters and other important disclaimers and information.

Sennheiser is a trademark of Texas Instruments.
All other trademarks are the property of their respective owners.

1 Key System Specifications

PARAMETER	SPECIFICATION
Supply Voltage	±2.5-V bipolar supplies
Quiescent Current	6 mA. This includes both channels on the stereo board.
Low-Power Mode	42 μ A. This includes both channels on the stereo board.
Maximum DAC Output Common Mode	1.8 V
Total System Gain	1 V/V (0 dB)
Target Headphone Load	32 Ω
Target Output Load	30 mW
THD+N	0.0003%, 20-Hz to 20-kHz measurement bandwidth, A-weighted
Idle Channel Noise	2 μ V _{RMS} (114 dBV), 20-Hz to 20-kHz measurement bandwidth, A-weighted

2 System Description

Figure 1 shows the complete schematic of the laboratory setup and the audio-amplifier signal chain. The output of the digital-to-analog converter (DAC) is modeled as a differential voltage with each output having 40-Ω output impedance. The output of the DAC drives the OPA1632 level-shift circuit that alters the common-mode offset of the differential DAC signal. The level-shift circuit drives the audio-amplifier board, which has two copies of the amplifier circuit, shown in Figure 1, for evaluation of stereo signals. The board is equipped with a headphone jack to evaluate the performance with different headphones.

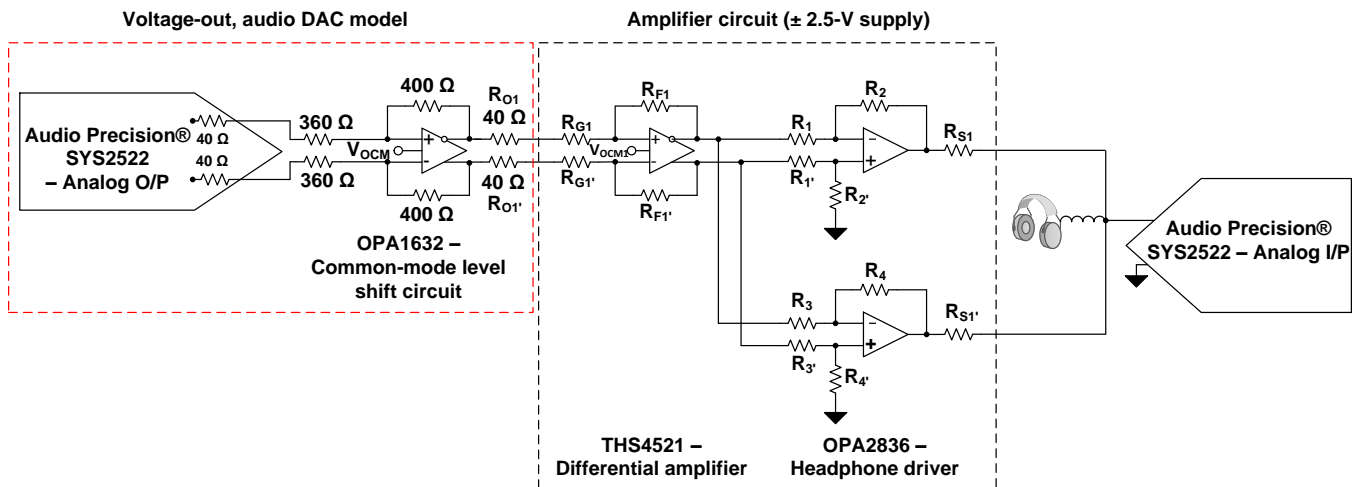


Figure 1. Block Diagram of System Used During Evaluation

2.1 OPA1632 Level-Shift Circuit

The Audio Precision 2522 cannot produce a differential output signal with an adjustable common-mode voltage. Instead, a fully differential amplifier in a unity-gain configuration is used to level-shift the common-mode voltage. The adjustable level shift is needed because audio DACs differ in their output common-mode voltages.

The OPA1632 was chosen for the adjustable level-shift because of its excellent audio characteristics and its ability to reproduce the signal from the Audio Precision 2522 with negligible signal degradation. The OPA1632 is operated on ± 15 -V supplies to maximize headroom and minimize distortion. The V_{OCM} pin is connected to an internal resistor-divider circuit, which defaults to mid-supply when left floating. To vary the output common mode from the OPA1632, its power supply rails are shifted asymmetrically around 0 V. The output common mode of the OPA1632 is always at mid-supply for optimum performance. The feedback resistors of the OPA1632 are set to 400 Ω as recommended in the data sheet. Resistors R_{O1} (and R_{O1}') in Figure 1 are set to 40 Ω to mimic the output resistance of the Audio Precision analog outputs. Mimicking the outputs inserts the OPA1632 into the signal chain without altering the total circuit gain.

2.2 THS4521 Differential Amplifier Stage

The THS4521 amplifies the output of the audio DAC and also shifts the common-mode voltage to ground for the subsequent headphone driver stage. An alternative is to use two parallel single-ended amplifiers, but a fully differential amplifier (FDA) has several performance advantages including:

- Superior HD2 performance. The architecture of the FDA provides inherent HD2 performance benefits compared to its single-ended opamp counterparts. In addition, each single-ended output of the FDA only needs half the voltage swing to produce the same differential output swing as a single-ended amplifier.
- Separate common-mode and differential gains- The differential gain, in case of a fully-differential input, is $-R_F/R_G$. The output common-mode voltage is independently controlled with the V_{OCM} pin, making it independent of the common-mode voltage of the input and also of the differential gain.
- Improved noise performance. Any noise from GND or the power supplies is automatically rejected by the FDA due to its differential architecture.

More information on FDAs can be found in *Fully-Differential Amplifiers Application Note* ([SLOA054D](#)). [Figure 2](#) shows the block diagram.

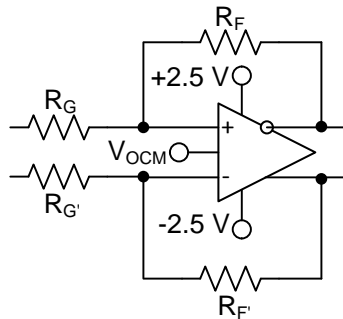


Figure 2. THS4521 FDA Block Diagram

2.3 OPA2836 Headphone Driver Stage

The function of the OPA2836 is two-fold:

1. Convert the differential output signal from the THS4521 to a single-ended signal.
2. Drive the headphone load.

The OPA2836 is available in a dual-channel 2x2-mm package that facilitates an extremely compact design for portable applications. The device also features an excellent performance-to-power ratio, making it an ideal choice for high dynamic-range audio applications.

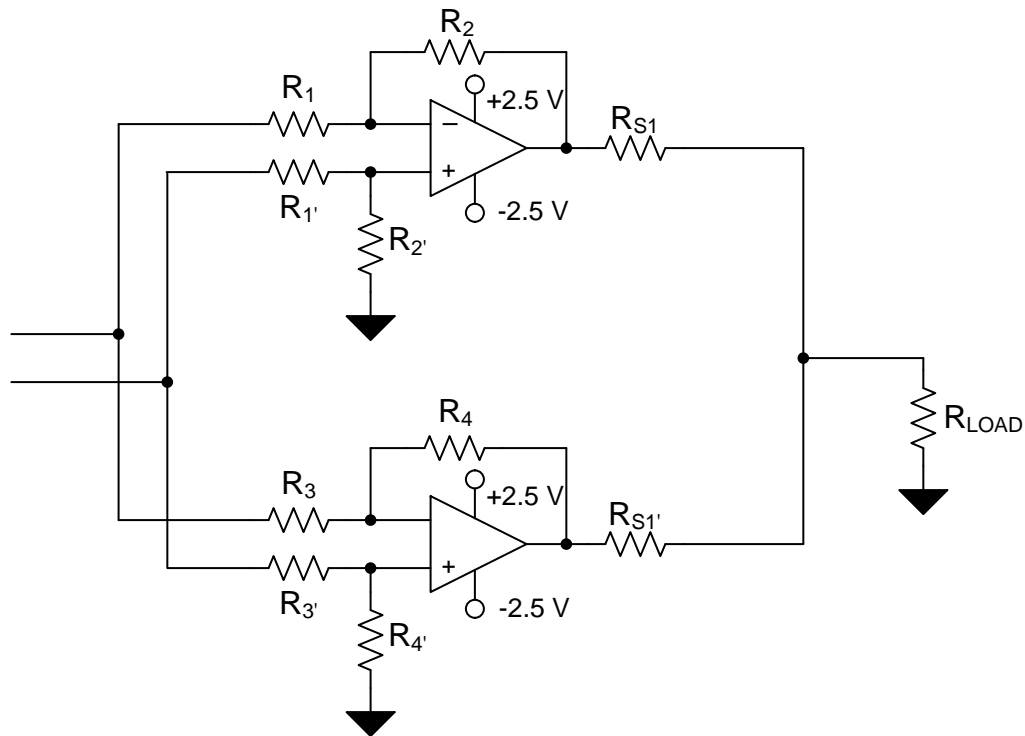


Figure 3. OPA2836 Driver Stage

Table 1. Key Specifications of OPA2836 and THS4521

DEVICE	QUIESCENT CURRENT (mA)	GBW (MHz)	SLEW RATE (V/μs)	BROADBAND NOISE (nV/√Hz)	HD2/HD3 at 100 kHz (dBc)
OPA2836	1.0	118	560	4.6	-133/-140
THS4521	1.0	93	490	4.6	-133/-141

2.4 System Design Options and Tradeoffs

For the specifications listed in [Table 1](#), the OPA2836 and THS4521 are quite similar, which creates interesting design trade-off considerations. The targeted signal chain gain is 1 V/V, which can be achieved in three ways:

- Gain of THS4521 = 1 and Gain of OPA2836 = 1
- Gain of THS4521 > 1 and Gain of OPA2836 = 1/(Gain of THS4521)
- Gain of THS4521 < 1 and Gain of OPA2836 = 1/(Gain of THS4521)

The output noise of a cascaded buffer stage is given by

$$V_{N_OUT} = \sqrt{(A_{VS2} \times (A_{VN1} \times N1))^2 + (A_{VN2} \times N2)^2}$$

, where A_{VN1} and A_{VN2} are the noise gains of each stage, $N1$ and $N2$ are the voltage-noise densities of each stage, and A_{VS2} is the signal gain of the second stage. From the equation, the gain should be concentrated in the first stage as the total noise from both stages is amplified by the gain of the second stage. The overall noise decreases as A_{VS2} is reduced. The second option in the previous list will provide the lowest noise.

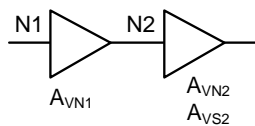


Figure 4. Cascaded Buffer Stage

Both amplifiers have similar distortion specifications, so the first two options yield similar distortion performance. In this application, the OPA2836 is driving the heavy headphone load, while the THS4521 is driving a much lighter load formed by the input resistors of the second stage. The heavy headphone load will degrade the distortion performance of the OPA2836. The architecture of the second option is the better choice, as it allows configuration of the OPA2836 with increased loop gain compared to the first option. While the second option appears to be the better choice, it is important to carefully determine the optimum gain of each stage. Increasing the gain of the first stage too much degrades performance due to swing limitations and reduced loop gain in the FDA. The THD+N performance of both options confirms that the second option is better.

The OPA2836 has a maximum linear output current drive of ± 45 mA, so the device can drive a 600- Ω headphone load with ease. However, to share the load when driving 32- Ω and 16- Ω , the second channel in the OPA2836 package is connected in parallel with the first channel.

The maximum offset voltage of the OPA2836 is specified as ± 400 μ V. If the outputs of the two amplifiers are directly connected, the differential offset voltage between the amplifiers causes a short and prevents the amplifiers from operating normally. To prevent the signals from shorting, a small series resistance $R_{S1} = R_{S1'} = 1$ Ω is inserted at the output of the each amplifier. The resistance serves to limit the current flow between the amplifier outputs. With these resistors in place, the worst-case DC current between the amplifier outputs is $(800$ μ V / 2 Ω) = 400 μ A.

An audio jack on the board enables testing with headphones; however, the results shown before [Section 5.3](#) are with a 32.4- Ω resistive load.

To validate these conclusions about the gain of each stage, two configurations were chosen for further evaluation. The values in Table 2 were chosen based on the components in Figure 1.

Table 2. Resistance Values for Each Gain Configuration

GAIN CONFIGURATION ($G_{\text{THS4521}} - G_{\text{OPA2836}}$) (V/V)	R_{G1} (and $R_{G1'}$) Ω ⁽¹⁾	R_{F1} (and $R_{F1'}$) Ω	R_1 and R_3 ($R_{1'}$ and $R_{3'}$) Ω	R_2 and R_4 ($R_{2'}$ and $R_{4'}$) Ω
1.50-0.67	698	1110	1110	741
1.00-1.00	1110	1110	1110	1110

⁽¹⁾ There is an additional 40 Ω of resistance from the previous stage: OPA1632 circuit or Audio Precision

The resistors used in this design have a tolerance of 0.1% that facilitates cancellation of even-order harmonic distortion in the FDA stage. The design of the resistors also maximizes the common-mode rejection in the differential-to-single-ended amplifier stage. Wherever possible, the capacitors used in the reference design are of the COG/NOP type ceramic. These capacitors have small voltage coefficients, which reduces distortion when large voltages are applied across them. More information can be found in [Signal Distortion from High-K Ceramic Capacitors](#) and [More About Understanding the Distortion Mechanism of High-K MLCCs](#).

3 Simulations

The schematic shown in Figure 5 is used to simulate noise and verify the DC and transient behavior of the audio circuit. Two voltage-controlled voltage sources (VCVs) are used to emulate the source of Audio Precision.

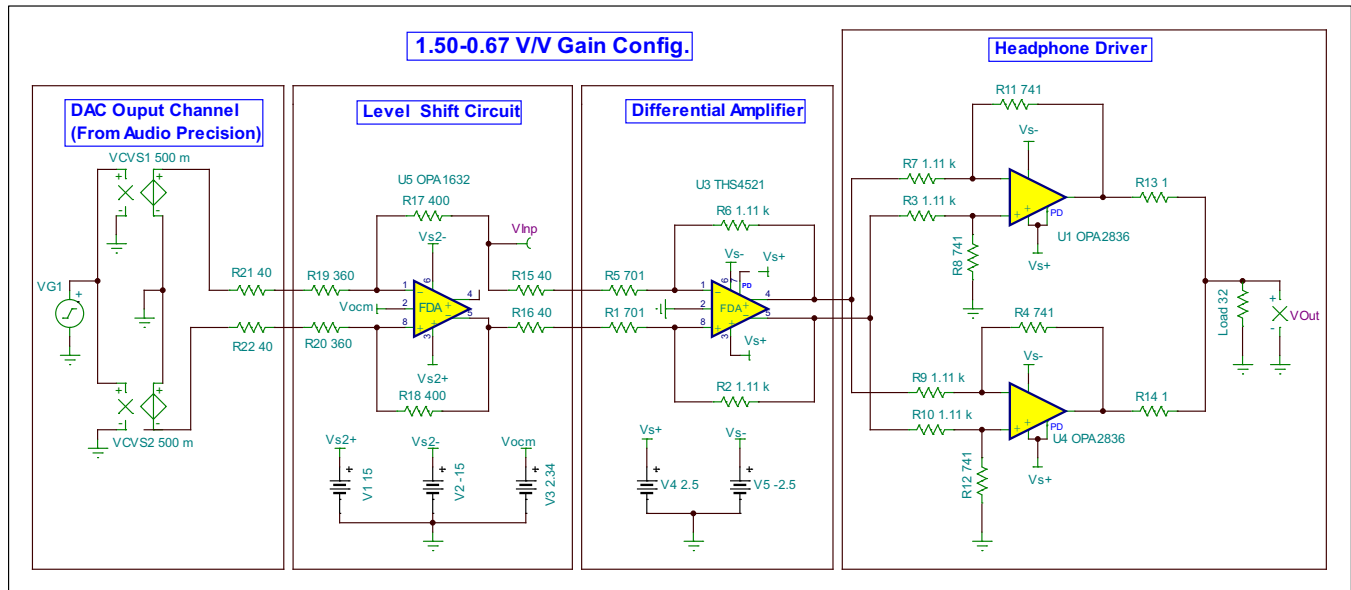


Figure 5. TINA Schematic of System

3.1 Noise

The idle-channel noise for both gain configurations was simulated. The OPA1632 was excluded from the system for this simulation. The inputs of the THS4521 stage were directly connected to the DAC output, and the total noise was simulated over a noise-bandwidth of 22 Hz to 22 kHz, as shown in Figure 6. From the results in Figure 6, the idle-channel noise for the 1-1 V/V (option a) and 1.50-0.67 V/V (option b) configurations were $2.30 \mu\text{V}_{\text{RMS}}$ and $1.85 \mu\text{V}_{\text{RMS}}$, which corresponds to -112.76 and -114.66 dBV, respectively. The current TINA-TI models are unable to simulate distortion, so THD+N was only measured and not simulated.

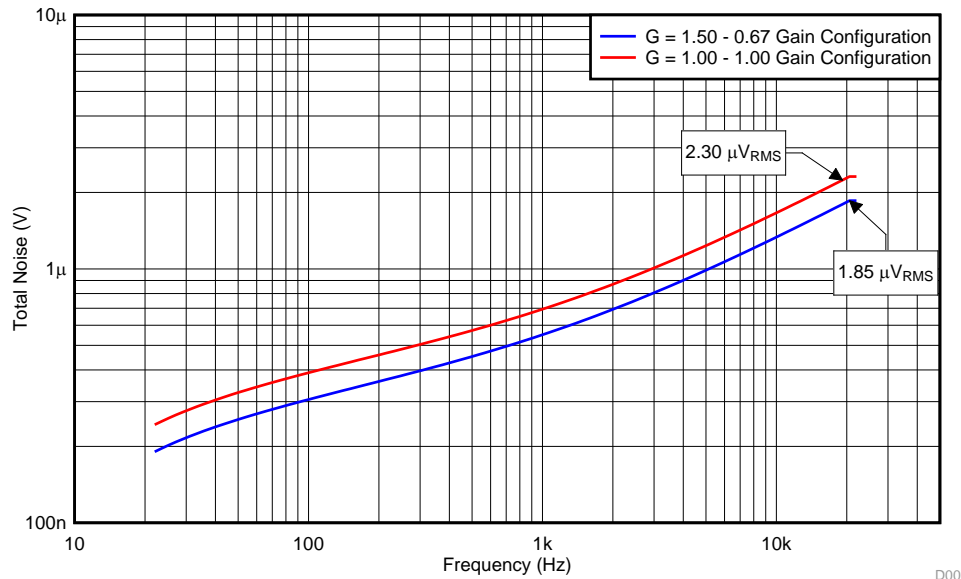


Figure 6. Simulated Output Noise in Both Gain Configurations

3.2 DAC Output Common-Mode Range

Both gain configurations were simulated while varying the input common-mode voltage. The input (R_{G1}) and feedback (R_{F1}) resistors of the FDA stage act as a voltage divider between the output common-mode voltage of the DAC and the output common-mode voltage of the FDA. The output DC offset of the THS4521 is set to mid-supply. From the THS4521 data sheet, the common-mode input voltage high limit is 3.6 V when the supplies are 0 V and 5 V, respectively. For ± 2.5 -V supplies, the common-mode input voltage high limit is 1.1-V. Equation 1 determines the maximum output common-mode voltage of the DAC that will not exceed the maximum input common-mode voltage of the THS4521.

$$V_{\text{CM_MAX(DAC)}} = \frac{V_{\text{CM_MAX(FDA)}}(R_F + R_G)}{R_G} \tag{1}$$

From Equation 1, Equation 2 and Equation 3 the maximum DAC common-mode voltage for the different gain configurations.

$$V_{\text{CM,1-1V/Vgain}} = \frac{1.1 \text{ V} (1.11 \text{ k}\Omega + 1.11 \text{ k}\Omega + 40 \text{ }\Omega)}{1.11 \text{ k}\Omega} = 2.24 \text{ V} \tag{2}$$

$$V_{\text{CM,1.50-0.67V/Vgain}} = \frac{1.1 \text{ V} (1.11 \text{ k}\Omega + 701 \text{ k}\Omega + 40 \text{ }\Omega)}{1.11 \text{ k}\Omega} = 1.83 \text{ V} \tag{3}$$

These calculations show that the input common-mode range of the THS4521 is reduced as its gain is increased, which limits the maximum gain setting of the THS4521 stage.

4 PCB Design

Figure 7 and Figure 8 show the PCB layout and schematic, respectively. The bill of materials (BOM) can be found in Table 5. To maximize performance, minimize trace lengths to reduce parasitic trace resistance, and ensure those trace lengths match.

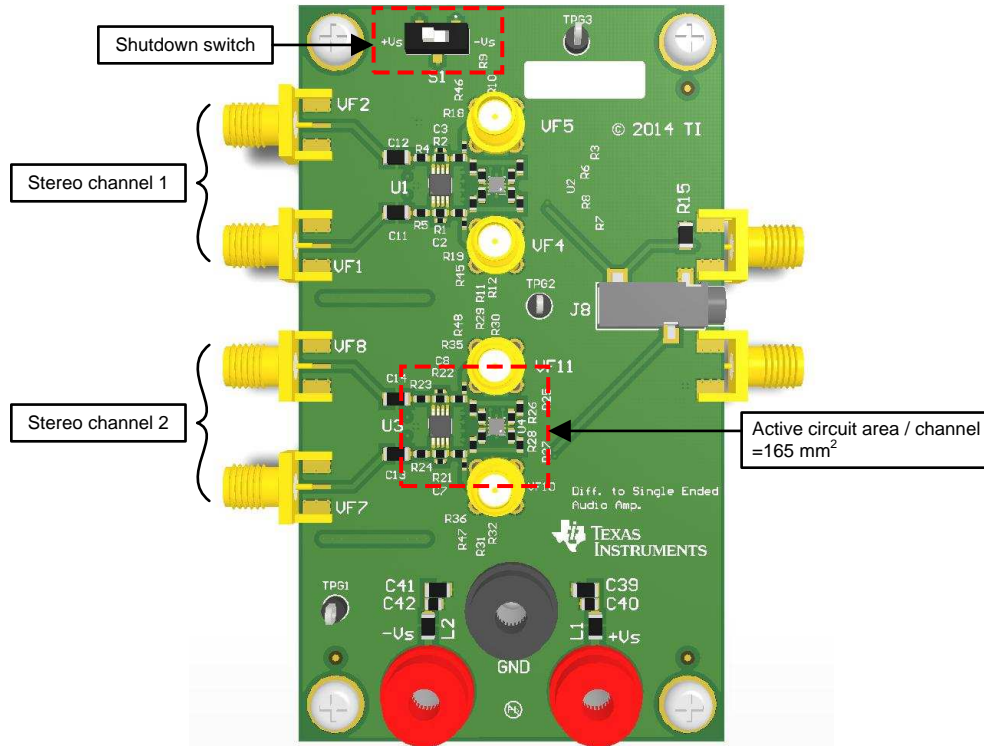


Figure 7. Audio Board PCB

4.1 Schematic

Figure 8 shows the Audio Board Circuit schematic.

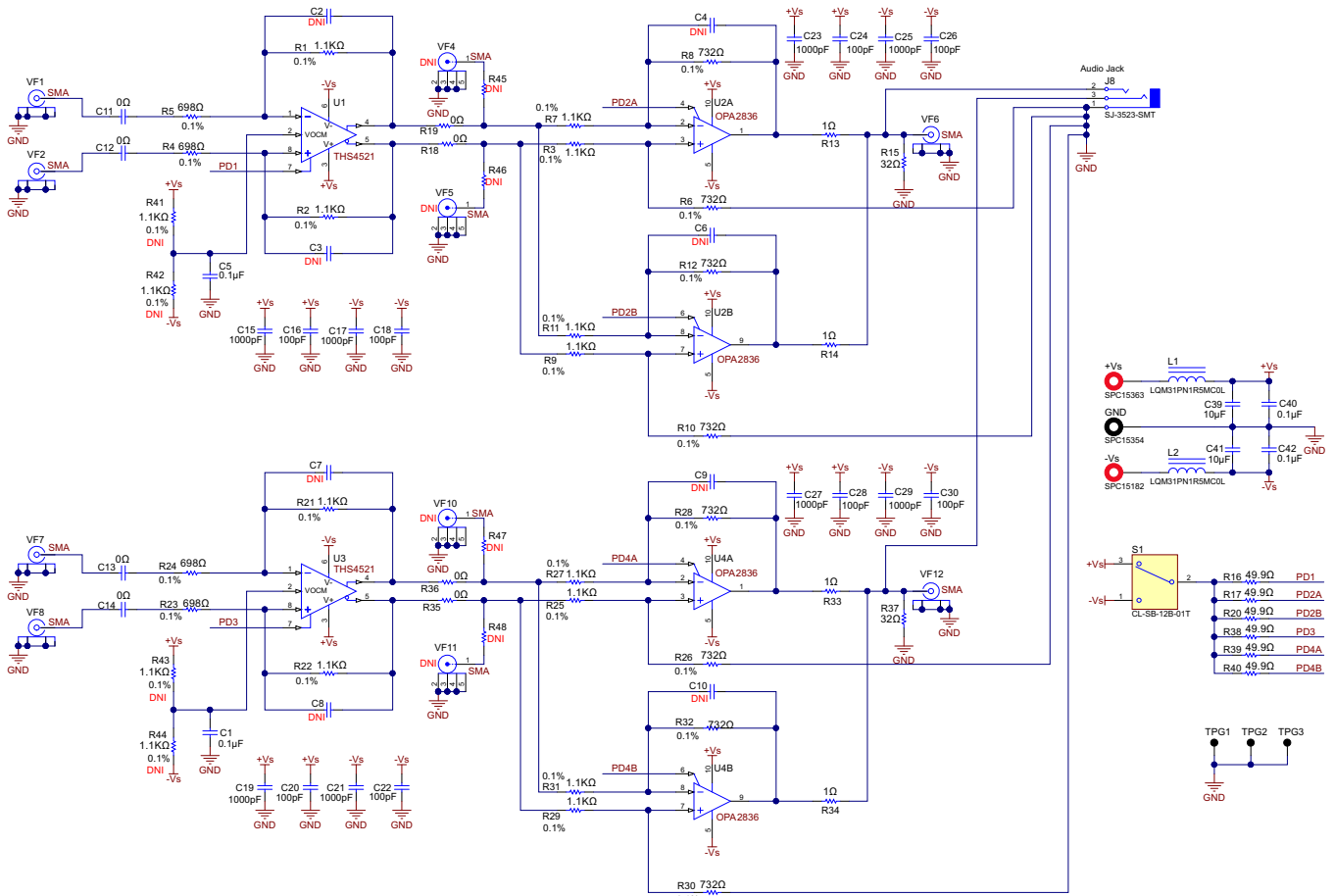


Figure 8. TIDA-00715 Audio Board Circuit Schematic

5 Verification and Measured Performance

Figure 9 shows the bench setup used to measure the performance of the audio board. Two triple-output power supplies are used to power both the OPA1632 level-shift circuit and the audio reference board. A PC is used to control the Audio Precision AP2522 interface and retrieve output data. The Audio Precision A-weighting filter option is enabled, and the measurement bandwidth is set to 20 Hz to 24 kHz for all measurements in this section.

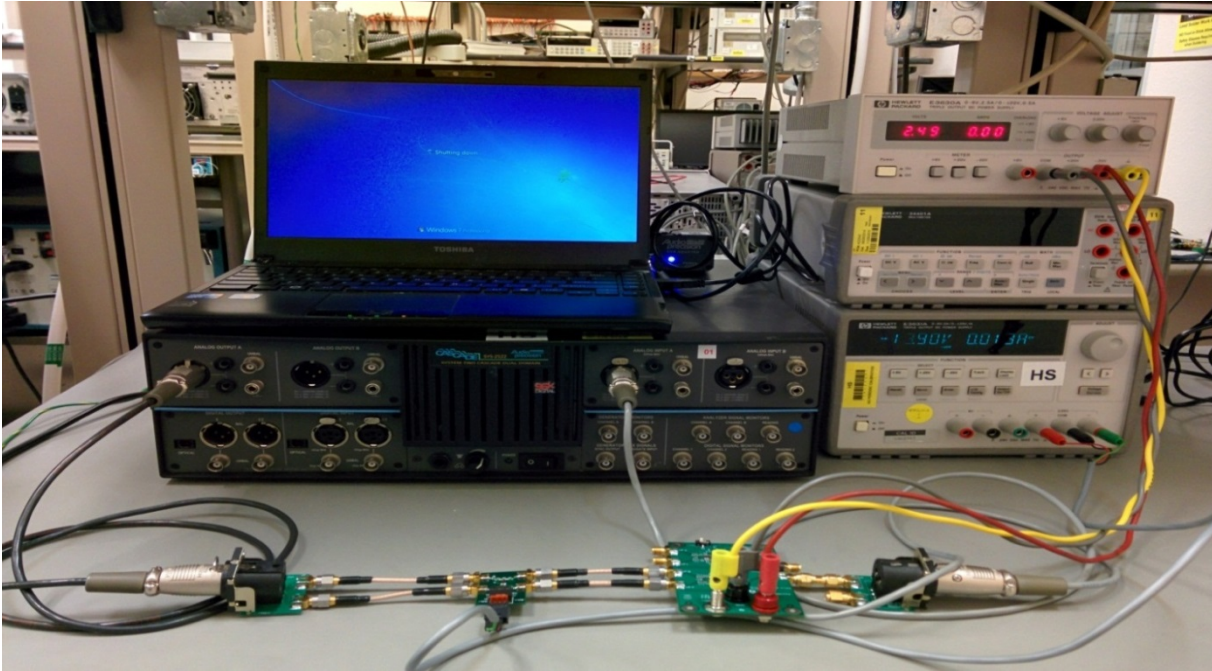


Figure 9. Laboratory Bench Setup Showing Audio Precision, OPA1632, and Audio Reference Board

5.1 Quiescent Current

One of the main benefits in this amplifier design is its power-to-performance ratio. Both the THS4521 and the OPA2836 typically consume 1.0 mA per channel, resulting in a typical quiescent power consumption of 15 mW for each channel of a stereo amplifier. The maximum quiescent power per channel of the stereo amplifier is 18.25 mW. Both the THS4521 and OPA2836 can be placed in shutdown mode and consume less than 11.5 μ A per channel. A switch is included on the audio reference board to control the state of the shutdown pins.

5.2 AP2522 and OPA1632 Level-Shift Circuit Baseline Performance

To estimate the performance of the audio board, baseline measurements of the AP2522 and OPA1632 level-shift circuit are made to ensure that the setup is not the limiting factor in the system measurements. The THD+N baseline measurement is shown in Figure 10 for a 1-kHz signal. The results in Figure 10 set a minimum for best system performance expected when testing with and without the OPA1632 circuit. The OPA1632 does cause some signal degradation. The x-axis in the figure is in watts, referred to a 32-Ω load. There is no load connected to the system for this measurement. The 32-Ω load is assumed for compatibility with the measurements in Section 5.3 and Section 5.4.

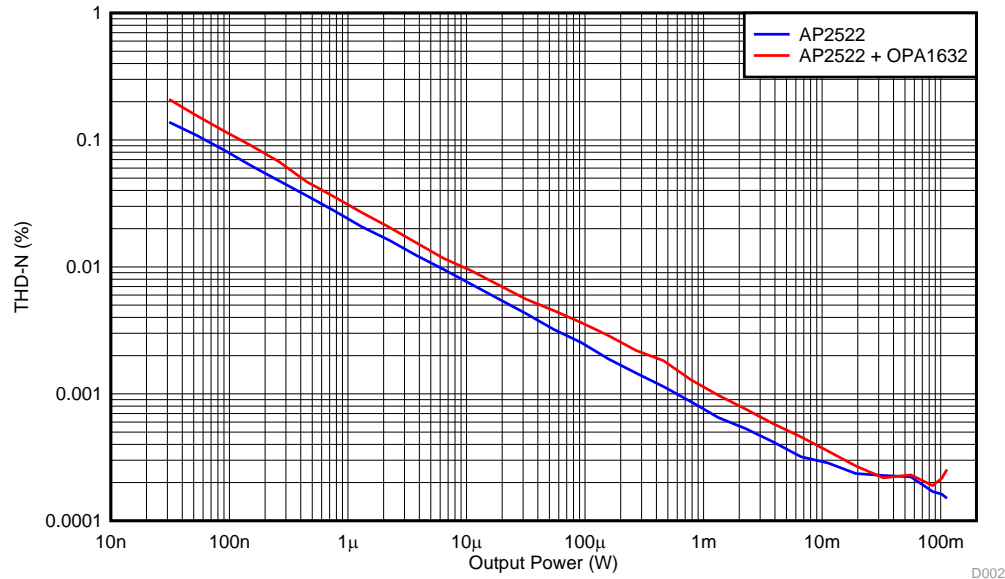


Figure 10. Baseline THD+N Performance of AP2522 and OPA1632

Figure 11 shows the baseline Fast Fourier Transform (FFT) performance when driving a 2- V_{PP} signal out of the AP2522. The low-frequency spurs are due to 60-Hz noise from the supplies.

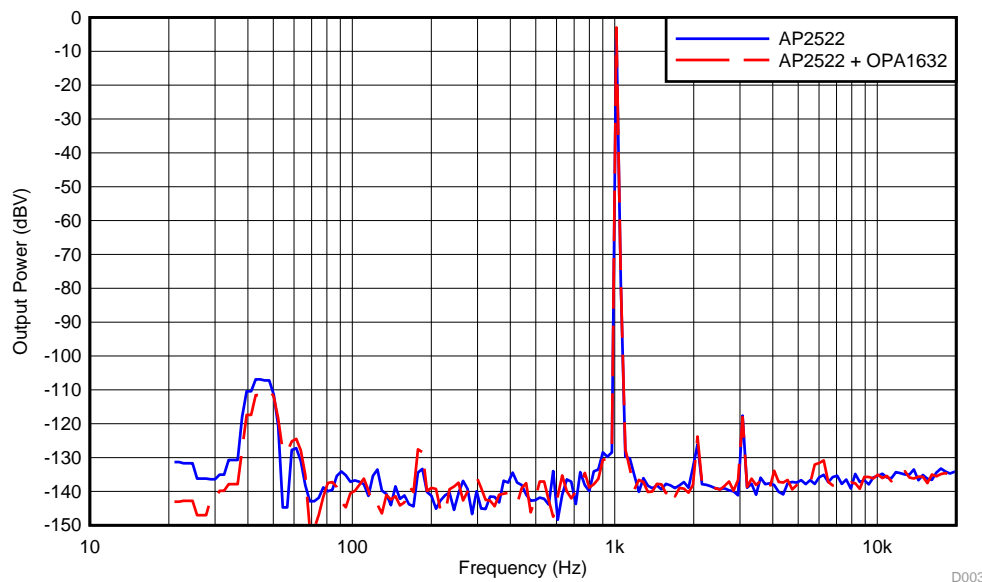


Figure 11. 1-kHz Baseline FFT, $V_{OUT} = 2 V_{PP}$

5.3 Audio Board Performance With 32-Ω Resistive Load

Measurements in this section are made with a 32-Ω resistive load with the A-weighting filter option of the Audio Precision enabled. The measurement bandwidth is set in the range of 20 Hz to 24 kHz.

5.3.1 Idle Channel Noise

[Table 3](#) compares the simulated and measured idle-channel noise levels for both gain configurations. The values for both cases are closely matched.

Table 3. Comparing Simulated and Measured Total Output Noise

GAIN CONFIGURATION ($G_{\text{TMS4521}} / G_{\text{OPA2836}}$) (V/V)	SIMULATED IDLE CHANNEL NOISE (dBV)	MEASURED IDLE CHANNEL NOISE (dBV)
1.00–1.00	–112.76	–113.532
1.50–0.67	–114.66	–115.605

5.3.2 THD+N vs Output Power With Variation in DAC Output Common-Mode Voltage

Figure 12 and Figure 13 show the 1-kHz, THD+N versus output power for both gain configurations as a function of the input common-mode voltage to the audio board. The 1-1 V/V gain setup allows for a wider input common-mode range at the cost of THD+N performance. From Section 3.2, the theoretical maximum common-mode voltage into the audio board for the 1-1 V/V gain configuration is 2.24 V. As shown in Figure 12, the common-mode voltage can be about 40% higher with minimal change in performance.

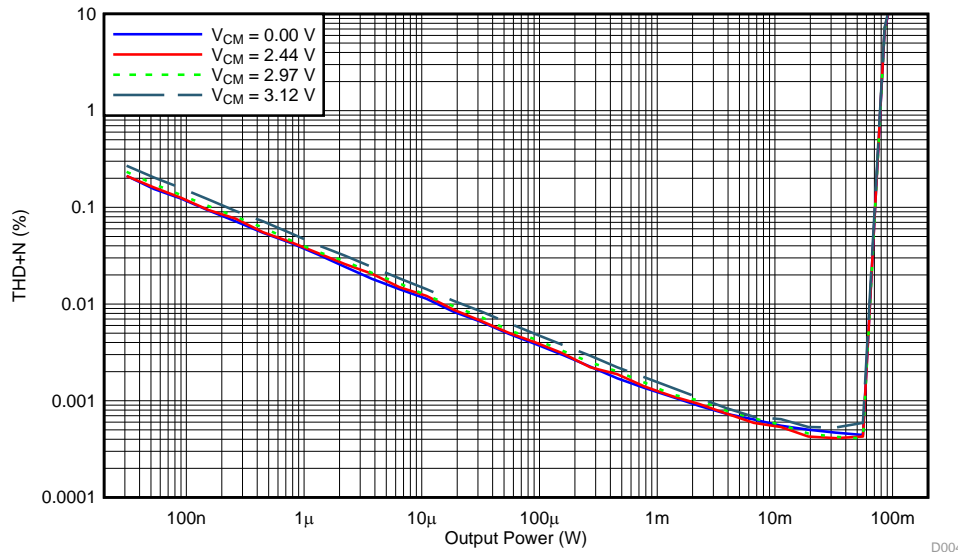


Figure 12. G = 1-1 V/V Config, 1-kHz In, THD+N vs Output Power vs. DAC Output Common-Mode

Similarly, from Figure 13 for the 1.50-0.67 V/V gain configuration, there is minimal difference in THD+N performance when the input common-mode range is increased by 40% beyond the calculated limit. Comparing Figure 12 with Figure 13, the 1-1 V/V gain configuration can deliver more power to the load at the cost of slightly degraded THD+N performance, indicating that the THS4521 is probably the limiting factor to the system THD+N performance. The higher closed-loop gain of the THS4521 in the 1.50-0.67 V/V gain configuration experiences headroom limitations at a lower output power compared to the 1-1 V/V gain configuration which degrades the amplifiers distortion. In the region with low output power where noise is dominant, one sees the benefit of the 1.50-0.67 V/V gain configuration.

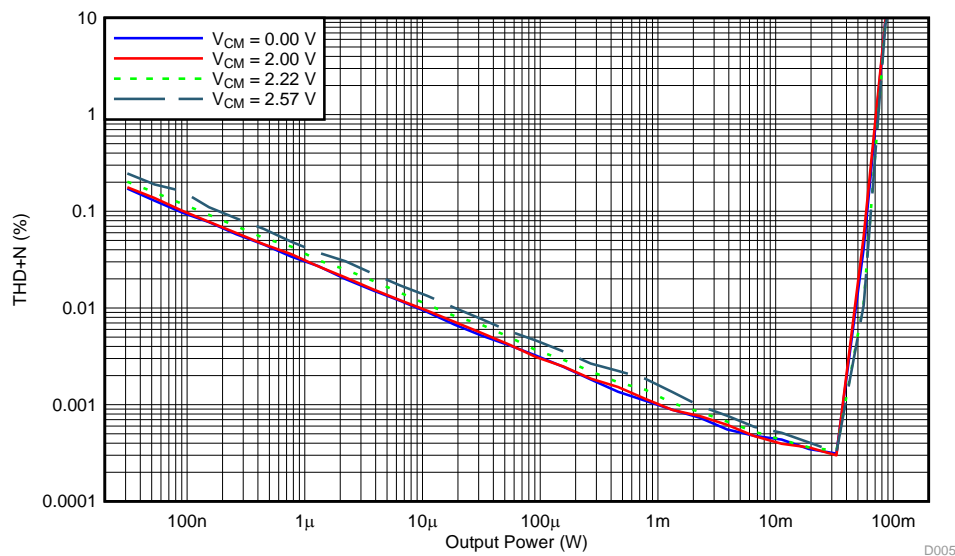


Figure 13. G = 1.50-0.67 V/V Config, 1 kHz In, THD+N vs Output Power DAC Output Common-Mode

5.3.3 Output Spectrum vs Variation in DAC Output Common-Mode Voltage

Figure 14 and Figure 15 show the 1-kHz output spectra for the two gain configurations as a function of the DAC output common-mode voltage. The output power is 15.6 mW ($2\text{-}V_{pp}$ output) in these figures. Comparing these results with the idle-channel noise measurements in Table 3. Comparing these results with the measurements in Table 3, noise dominates the THD+N performance in the 1-1 V/V gain configuration.

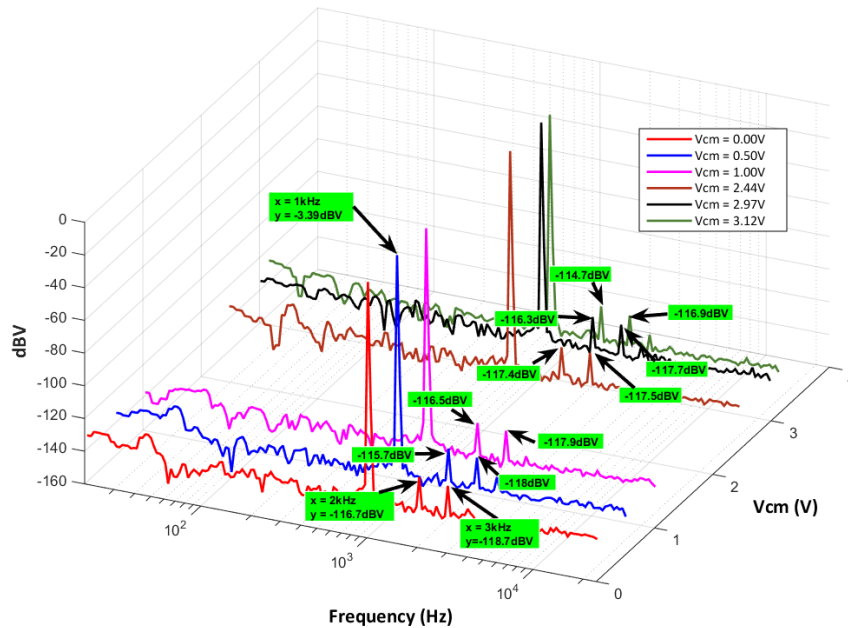


Figure 14. G = 1-1 V/V, HD vs DAC Output Common-Mode Voltage, $V_{OUT} = 2 V_{PP}$

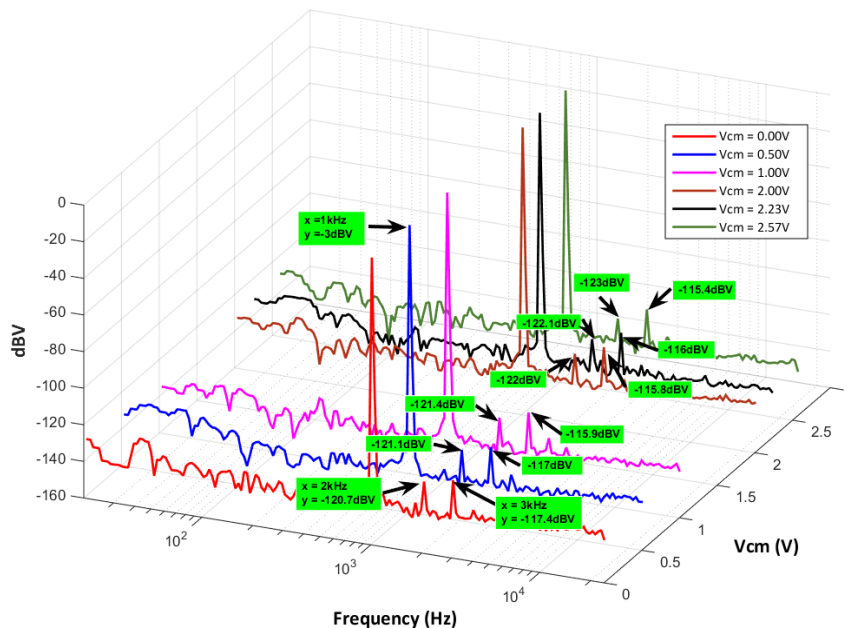


Figure 15. G = 1.5 - 0.67 V/V, HD vs DAC Output Common-Mode Voltage, $V_{OUT} = 2 V_{PP}$

In the case of the 1.5-0.67 V/V gain configuration, the noise and HD3 start to become the dominant factors; but since this setting has lower noise, the resultant THD+N performance is superior to the former gain configuration.

The HD2 performance for 1.5-0.67 V/V is also markedly superior to that of 1-1 V/V, indicating that the OPA2836 is the dominant HD2 contributor. Thus, going to a higher loop gain in the driver stage improves the overall HD performance. The heavy load that the OPA2836 is driving results in the power supplies becoming contaminated by HD2 components. The output stage of the OPA2836 has a class-AB configuration; hence, during each half-cycle of a sine-wave, one side of the output stage is providing all of the current, inducing a half-wave rectified load current in the output stage of the amplifier, which degrades the HD2. HD3 performance is limited by the AP2522 + OPA1632 as shown in [Figure 11](#).

5.3.4 Pop-and-Click Response

Pop-and-click refers to spurious transient signal produced at the output of the headphone when the audio signal chain is either enabled or disabled. Large pop-and-click transients could undermine the commercial attractiveness of the product because it could cause irritation to the end user. The audio board is equipped with a switch that controls the Power Down (PD) pin of the THS4521 and OPA2836. The switch was used to enable and disable the audio board amplifiers in order to evaluate the pop-and-click response.

[Figure 16](#) shows the pop-and-click responses of the audio board with the audio board inputs grounded and with the A-weighting filter applied. Glitches of this magnitude will not cause any audible artifacts during enabling and disabling even for high-end headsets.

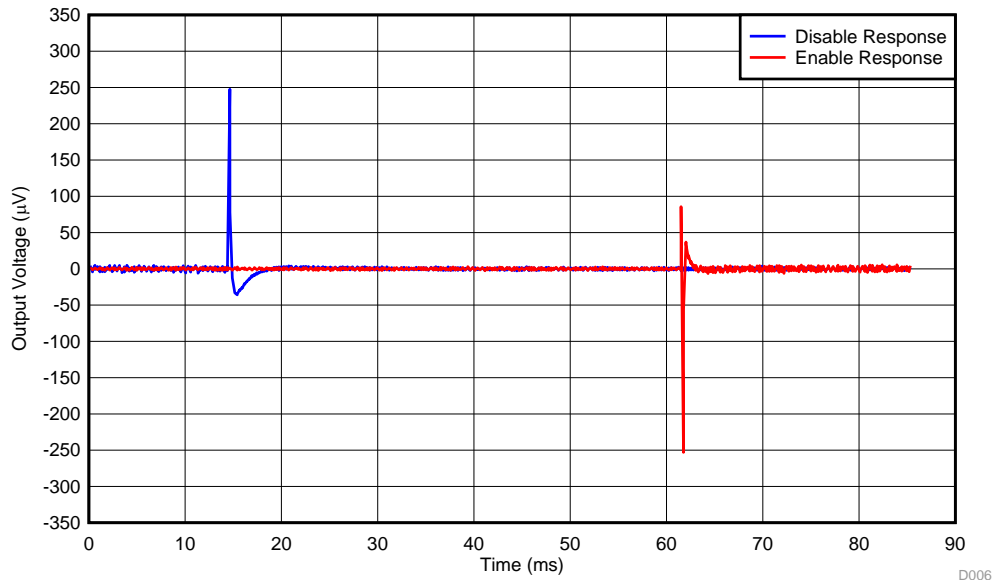


Figure 16. Pop-and-Click Response in G = 1.5-0.67 V/V Configuration

5.3.5 Multiplexed Operation

In certain applications (for example, portable with support for HiFi audio), having two separate signal paths may be desirable: a high-performance path and a low-power path where diminished signal quality is acceptable. In such situations a switch is typically inserted into the design to allow path selection. One benefit of the OPA2836 and THS4521 power-down mode is their ability to present a high output impedance when the mode is enabled, letting the end-user save BOM cost and board space by eliminating the need for the switch. Additionally, any nonlinearity introduced by the switch is also eliminated.

Tests were conducted in the lab to verify the performance of the audio board in a multiplexed configuration. The outputs of two similarly configured audio boards were shorted. One audio board had the inputs grounded while in power-down mode. The second audio board was in power-on mode with the inputs connected to the Audio Precision. The THD+N and output spectra were measured, and the results were compared with the standard single-board setup. Figure 17 and Figure 18 below do not show any discernable change in performance between the standard and multiplexed modes.

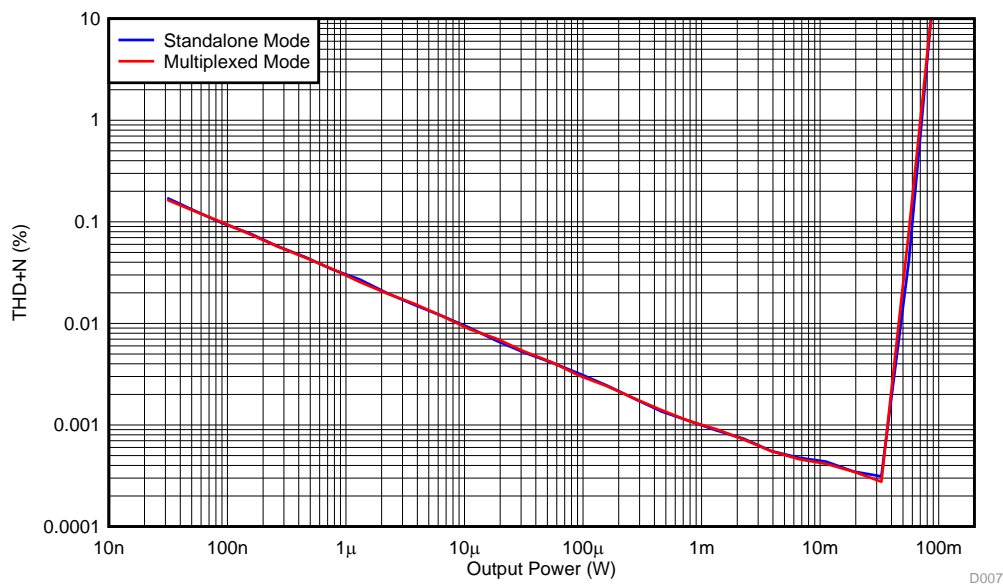


Figure 17. Stand-Alone vs Multiplexed Mode in $G = 1.5-0.67$ V/V Configuration (1 KHz)

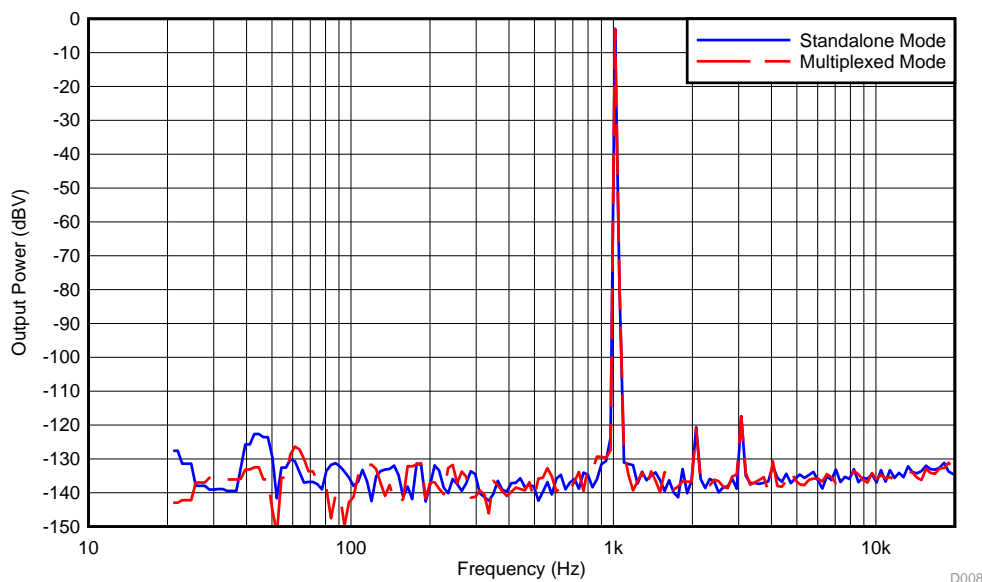


Figure 18. Stand-Alone vs Multiplexed Mode in $G = 1.5-0.67$ V/V Configuration, $V_{OUT} = 2 V_{PP}$

5.3.6 Performance With 16-Ω Resistive Load

The performance of the audio board was also verified using a 16-Ω resistive load. The heavier load degraded the distortion performance. At lower output-voltage swings where the load current requirements are less stringent, both load configurations displayed equivalent performance. Table 4 also shows that while the HD3 is slightly worse for the 16-Ω load compared to the 32-Ω load, the HD2 was significantly worse. This corroborates the statement in Section 5.3.4 that the load currents are the primary determinant of the HD2 performance of the OPA2836. Figure 19 and Figure 20 show 16 Ω vs 32 Ω, THD+N performance, ($G = 1.5 - 0.67 \text{ V/V}$) and 16 Ω vs 32-Ω, Output Spectrum, $V_{OUT} = 2 V_{PP}$ ($G = 1.5-0.67 \text{ V/V}$).

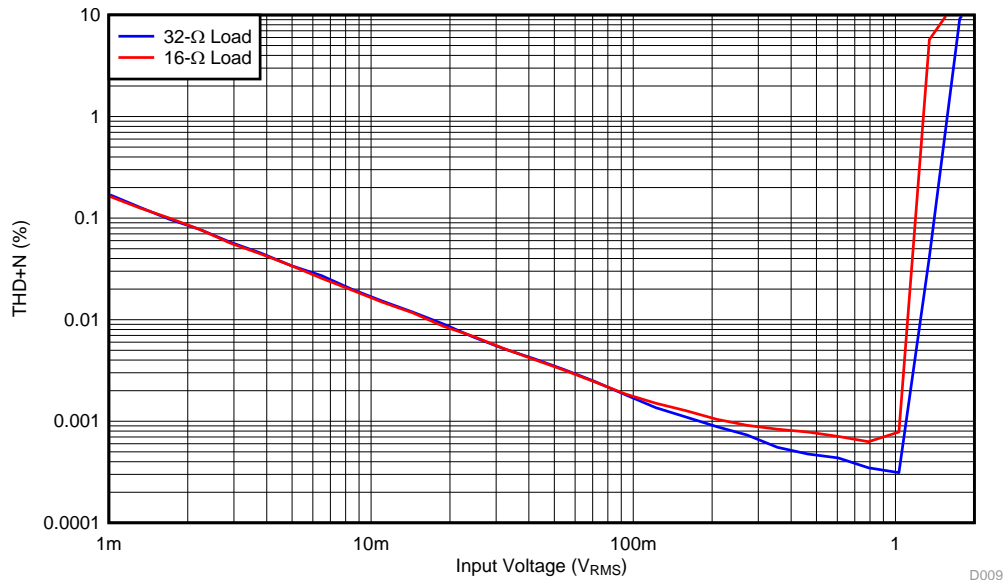


Figure 19. 16 Ω vs 32 Ω, THD+N Performance, ($G = 1.5-0.67 \text{ V/V}$)

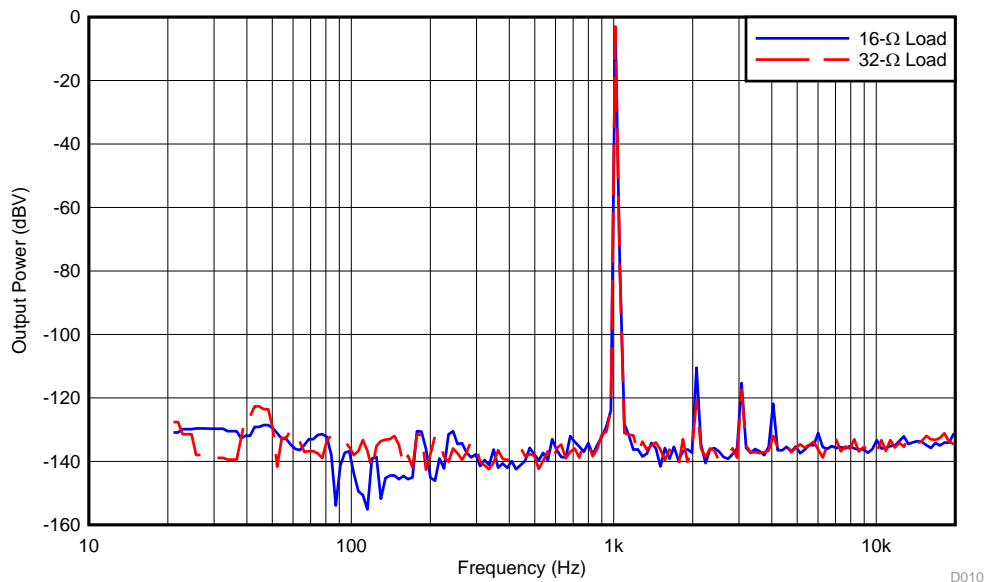


Figure 20. 16 Ω vs 32-Ω, Output Spectrum, $V_{OUT} = 2 V_{PP}$ ($G = 1.5-0.67 \text{ V/V}$)

Table 4. Comparing HD performance at Different Loads With 1 KHz, 2- V_{PP} Output ($G = 1.5-0.67 \text{ V/V}$)

RESISTIVE LOAD (Ω)	HD2 (dBc)	HD3 (dBc)
32	-120.7	-117.4
16	-110.5	-115.3

5.4 Audio Board Performance With 32-Ω Headphone Load

For all the previous results, resistive loads were used as standard setup. Headphones have a more complex impedance and cannot be accurately modeled as simple resistors. Headphone impedances are determined by the electrical characteristics of the voice coil, the magnetic coupling of the coil, and the headphone magnet. To characterize the performance of the audio board under more realistic conditions, a nominal 32-Ω impedance headphone, Sennheiser™ HD428, was used.

5.4.1 Performance at 1 kHz

The 32-Ω resistive load at the output of the amplifier was removed and the Sennheiser HD428 headphone was plugged into the audio jack. The design was retested under these conditions and compared with the original data. From Figure 21 and Figure 22, there is no discernable difference in performance when tested with a 1-kHz signal.

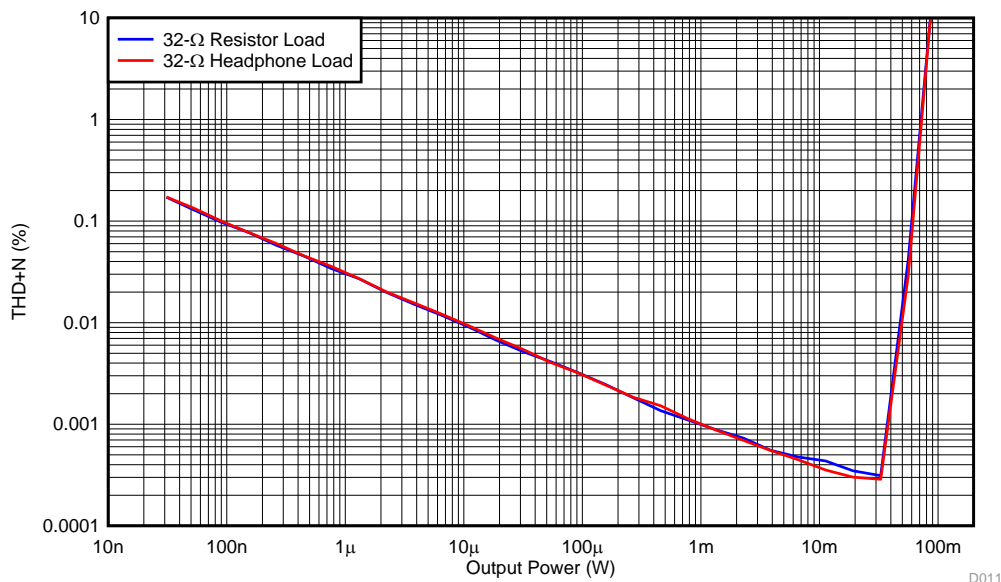


Figure 21. 32-Ω Headphone vs 32-Ω Resistor Load, THD+N Performance, (G = 1.5-0.67 V/V)

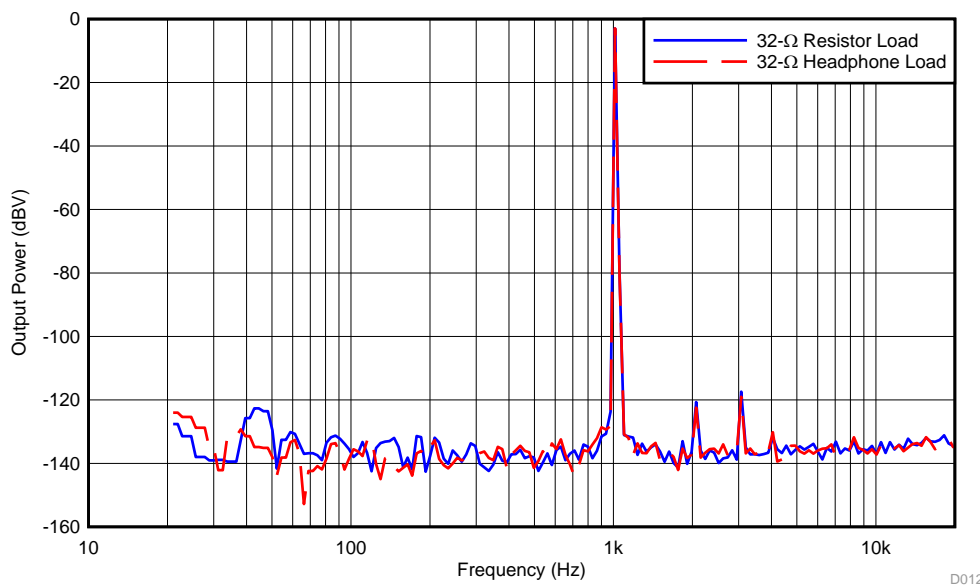


Figure 22. 32-Ω Headphone vs 32-Ω Resistor Load, Output Spectrum, $V_{OUT} = 2 V_{PP}$ (G = 1.5-0.67 V/V)

5.4.2 Pop-and-Click Response

Figure 23 shows the pop-and-click transient response of the audio board with the headphone connected to the amplifier output. The response looks similar to what was observed during the test with the 32- Ω load.

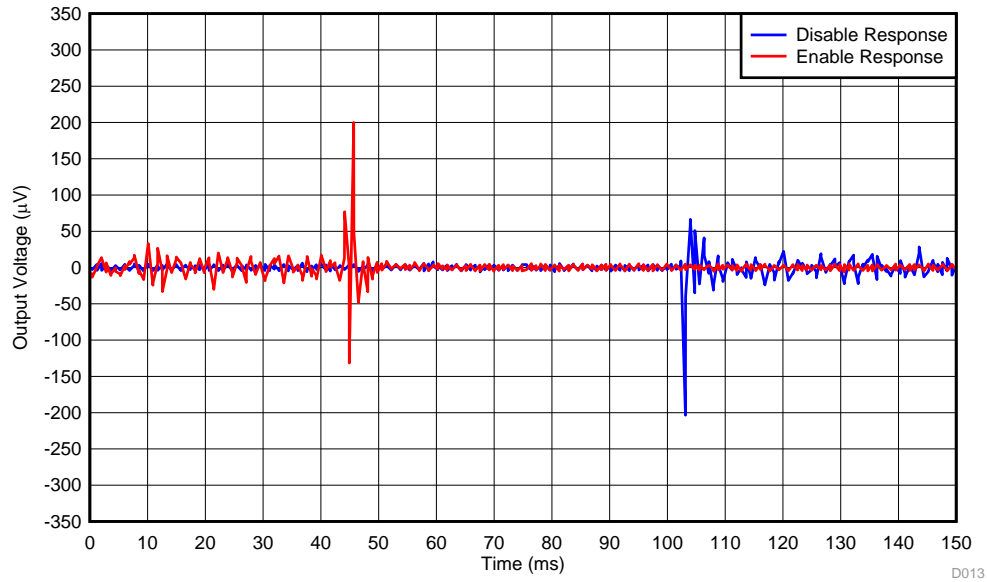


Figure 23. Pop-and-Click Transient Response of Audio Board With Headphone ($G = 1.5\text{-}0.67\text{ V/V}$)

5.4.3 Linearity Performance vs Frequency Using 32-Ω Headphone Load

Previously, the complex impedance profile of a headphone was mentioned. [The Sonic Advantages of Low-Impedance Headphone Amplifiers](#) gives a detailed explanation of the issues caused by the interaction between the output impedance of the amplifier and the headphone load. The performance of the audio board was measured across the audio spectrum with a 32-Ω resistor load and a headphone load. The 1.5-0.67 V/V gain configuration was used for this test with results shown in [Figure 24](#).

The headphone load produces higher nonlinearity at lower frequencies. The headphone impedance varies as a function of the instantaneous voltage across the coil at a given frequency, thus creating a nonlinear load. The nonlinear load introduces a subsequent nonlinear current through the coil. The nonlinear current flowing through R_{ISO} results in a voltage drop that is seen at the Audio Precision inputs.

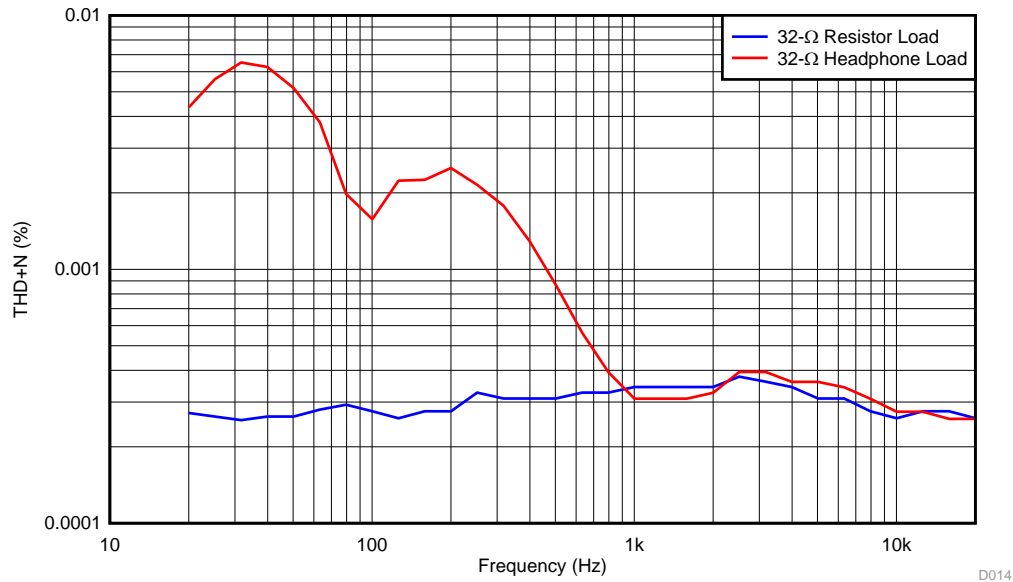


Figure 24. THD+N Performance vs Frequency (G = 1.5-0.67 V/V)

Figure 25 shows the circuit setup for the single drive channel.

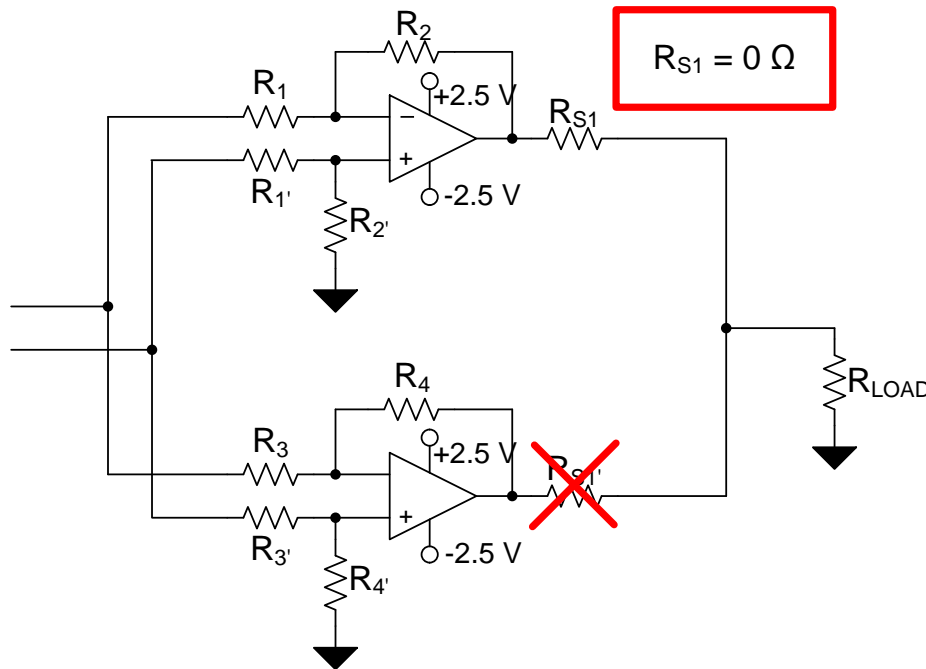


Figure 25. Circuit Setup for the Single Drive Channel

To verify the previous statements, the circuit was retested with only a single channel of the OPA2836 driving the headphone and setting R_{S1} to 0Ω , as shown in Figure 25. The result in Figure 26, shows a marked improvement in low-frequency THD+N performance, despite being driven by a single channel of the amplifier. The amplifier is still driving a nonlinear current into the headphone; however, because $R_{S1} = 0 \Omega$, there is no resultant voltage drop across the resistor as was observed in the previous case, proving that the nonlinearity is a result of the current through the headphone load rather than an inherent amplifier issue. The resultant audible nonlinearity will be present irrespective of the value of R_{S1} . From this result, one concludes that the dual-channel configuration with $R_{S1} = R_{S1}' = 1 \Omega$ will produce the best audio distortion performance.

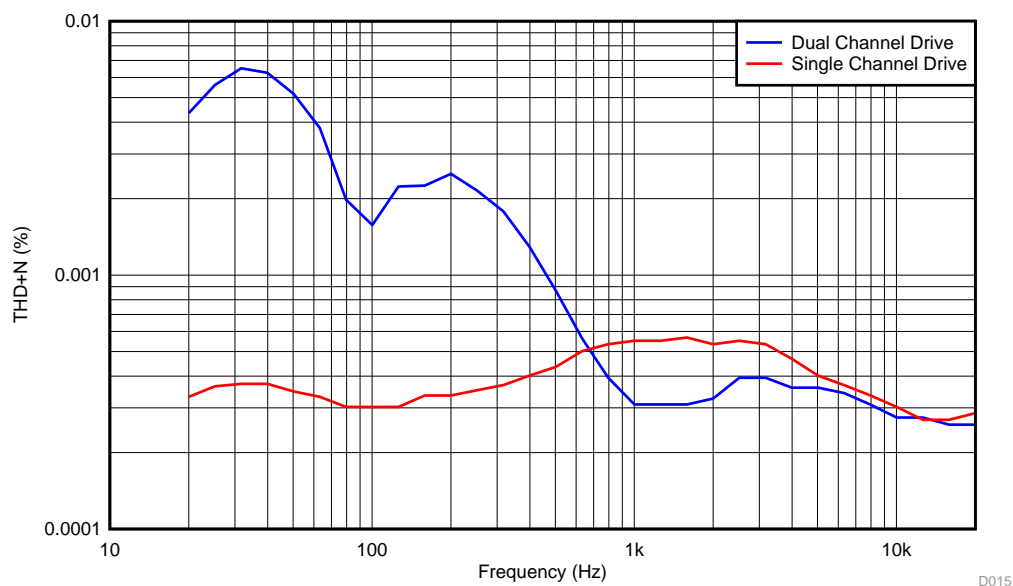


Figure 26. Single vs Dual-Channel THD+N vs Frequency, $V_{OUT} = 2 V_{PP}$ ($G = 1.5-0.67 V/V$)

6 Conclusion

This reference design explores various options and tradeoffs to consider when optimizing a circuit for a headphone-driver application. It demonstrates the excellent linearity performance of the OPA2836 and THS4521 and their best-in-class performance-to-power ratio.

7 Design Files

7.1 Bill of Materials

To download the bill of materials (BOM), see the design files at [TIDA-00715](http://www.ti.com/lit/zip/TIDA-00715).

Table 5. Bill of Materials

DESIGNATOR	QTY	VALUE	DESCRIPTION	PACKAGE REFERENCE	PART NUMBER	MANUFACTURER
+Vs	1		Banana Jack, Solder Lug, Red, Th	Red Insulated Banana Jack	SPC15363	Tenma
-Vs	1		Banana Jack, Solder Lug, Green, Th	Green Insulated Banana Jack	SPC15182	Tenma
C1, C5	2	0.1 μ F	CAP, CERM, 0.1 μ F, 50 V, \pm 10%, X7R, 0603	0603	C1608X7R1H104K	TDK
C11, C12, C13, C14	4	0 Ω	RES, 0, 5%, 0.25 W, 1206	1206	CRCW12060000Z0EA	Vishay-Dale
C15, C17, C19, C21	4	1000 pF	CAP, CERM, 1000 pF, 50 V, \pm 5%, C0G/NP0, 0603	0603	C1608C0G1H102J	TDK
C16, C18, C20, C22	4	100 pF	CAP, CERM, 100 pF, 50 V, +/- 5%, C0G/NP0, 0603	0603	06035A101JAT2A	AVX
C23, C25, C27, C29	4	1000 pF	CAP, CERM, 1000 pF, 25 V, \pm 5%, C0G/NP0, 0402	0402	C1005C0G1E102J	TDK
C24, C26, C28, C30	4	100 pF	CAP, CERM, 100 pF, 50 V, \pm 5%, C0G/NP0, 0402	0402	CC0402JRNPO9BN101	Yageo America
C39, C41	2	10 μ F	CAP, CERM, 10 μ F, 25 V, \pm 10%, X5R, 1206	1206	GRM31CR61E106KA12L	MuRata
C40, C42	2	0.1 μ F	CAP, CERM, 0.1 μ F, 50 V, \pm 10%, X7R, 0805	0805	08055C104KAT2A	AVX
GND	1		Banana Jack, Solder Lug, Black, Th	Black Insulated Banana Jack	SPC15354	Tenma
H1, H2, H3, H4	4		Machine Screw, Round, #4-40 x 1/4, Nylon, Phillips pan-head	Screw	NY PMS 440 0025 PH	B&F Fastener Supply
H5, H6, H7, H8	4		Standoff, Hex, 0.5"L #4-40 Nylon	Standoff	1902C	Keystone
J8	1		Audio Jack, 3.5 mm, Stereo, R/A, SMT	Audio Jack SMD	SJ-3523-SMT	CUI Inc.
L1, L2	2	1.5 μ H	Inductor, Multilayer, Ferrite, 1.5 μ H, 1 A, 0.17 Ω , SMD	1206	LQM31PN1R5MCO L	MuRata
LBL1	1	1.11k	Thermal Transfer Printable Labels, 0.650" W x 0.200" H - 10,000 per roll	PCB Label 0.650" H x 0.200" W	THT-14-423-10	Brady
R1, R2, R3, R7, R9, R11, R21, R22, R25, R27, R29, R31	12	698	RES, 1.11 k, 0.1%, 0.1 W, 0603	0603	RT0603BRD071K11L	Yageo America
R4, R5, R23, R24	4	741	RES, 698, 0.1%, 0.1 W, 0603	0603	RT0603BRD07698RL	Yageo America
R6, R8, R10, R12, R26, R28, R30, R32	8	1.0	RES, 741, 0.1%, 0.1 W, 0603	0603	RT0603BRD07741RL	Yageo America
R13, R14, R33, R34	4	32.4	RES, 1.0, 5%, 0.1 W, 0603	0603	CRCW06031R00JNE A	Vishay-Dale
R15, R37	2	49.9	RES, 32.4, 1%, 0.25 W, 1206	1206	CRCW120632R4FKE A	Vishay-Dale
R16, R17, R20, R38, R39, R40	6	0	RES, 49.9, 1%, 0.063 W, 0402	0402	CRCW040249R9FKE D	Vishay-Dale
R18, R19, R35, R36	4		RES, 0, 5%, 0.1 W, 0603	0603	CRCW06030000Z0EA	Vishay-Dale
S1	1		Switch, Slide, SPDT, 0.2A, GULL, 12V, SMD	SMD, 3-Leads, Body 8.5 x 3.5mm, Pitch 2.5mm	CL-SB-12B-01T	Copal Electronics
U1, U3	2		VERY LOW POWER, NEGATIVE RAIL INPUT, RAIL-TO-RAIL OUTPUT, FULLY DIFFERENTIAL AMPLIFIER, DGK0008A	DGK0008A	THS4521DGK	Texas Instruments
U2, U4	2		Dual, Very Low Power, Rail to Rail Out, Negative Rail In, VFB Operational Amplifier, 2.5 to 5.5 V, -40 to 85 degC, 10-pin QFN (RUN0010A), Green (RoHS & no Sb/Br)	RUN0010A	OPA2836IRUNT	Texas Instruments

Table 5. Bill of Materials (continued)

DESIGNATOR	QTY	VALUE	DESCRIPTION	PACKAGE REFERENCE	PART NUMBER	MANUFACTURER
VF1, VF2, VF6, VF7, VF8, VF12	6	142-0711-821	CONNECTOR, SHEILDED, END LAUNCH JACK, GOLD PLATED, FOR 0.062 PCB, EDGE MOUNTED	0.250 SQ	142-0711-821	Cinch Connectivity Solutions Johnson
C2, C3, C4, C6, C7, C8, C9, C10	0		CAP, CERM, xxxF, xxV, [TempCo], xx%, [Package Reference]	0402		N/A
R41, R42, R43, R44	0	1.11k	RES, 1.11 k, 0.1%, 0.1 W, 0603	0603	RT0603BRD071K11L	Yageo America
R45, R46, R47, R48	0	0	RES, 0, 5%, 0.063 W, 0402	0402	CRCW04020000Z0ED	Vishay-Dale
TPG1, TPG2, TPG3	0	BLACK	Test Point, Multipurpose, Black, TH	Black Multipurpose Testpoint	5011	Keystone
VF4, VF5, VF10, VF11	0		Connector, TH, SMA	SMA	142-0701-201	Emerson Network Power

8 References

1. *Fully-Differential Amplifiers Application Note* ([SLOA054D](#))
2. *Caldwell, J. Signal Distortion from High-K Ceramic Capacitors*, <http://www.edn.com/design/analog/4416466/Signal-distortion-from-high-K-ceramic-capacitors>, 2013.
3. *Caldwell, J. More About Understanding the Distortion Mechanism of High-K MLCCs*, <http://www.edn.com/design/analog/4416466/Signal-distortion-from-high-K-ceramic-capacitors>, 2013.
4. *Siau, John. The Sonic Advantages of Low-Impedance Headphone Amplifiers*, <http://benchmarkmedia.com/blogs/white-papers/11653109-the-0-ohm-headphone-amplifier>, 2001.

9 About the Authors

HOA NGUYEN is a summer intern is a summer intern with Texas Instruments in the high-speed amplifier division in Tucson, AZ. He is currently working on his BSEE degree from Arizona State University.

SAMIR CHERIAN is an applications engineer with Texas Instruments in the high-speed amplifier division in Tucson, AZ. He is responsible for silicon evaluation of high-speed amplifiers as well as providing customer support through TI online forums, application notes, and reference designs.

IMPORTANT NOTICE FOR TI REFERENCE DESIGNS

Texas Instruments Incorporated ("TI") reference designs are solely intended to assist designers ("Buyers") who are developing systems that incorporate TI semiconductor products (also referred to herein as "components"). Buyer understands and agrees that Buyer remains responsible for using its independent analysis, evaluation and judgment in designing Buyer's systems and products.

TI reference designs have been created using standard laboratory conditions and engineering practices. **TI has not conducted any testing other than that specifically described in the published documentation for a particular reference design.** TI may make corrections, enhancements, improvements and other changes to its reference designs.

Buyers are authorized to use TI reference designs with the TI component(s) identified in each particular reference design and to modify the reference design in the development of their end products. HOWEVER, NO OTHER LICENSE, EXPRESS OR IMPLIED, BY ESTOPPEL OR OTHERWISE TO ANY OTHER TI INTELLECTUAL PROPERTY RIGHT, AND NO LICENSE TO ANY THIRD PARTY TECHNOLOGY OR INTELLECTUAL PROPERTY RIGHT, IS GRANTED HEREIN, including but not limited to any patent right, copyright, mask work right, or other intellectual property right relating to any combination, machine, or process in which TI components or services are used. Information published by TI regarding third-party products or services does not constitute a license to use such products or services, or a warranty or endorsement thereof. Use of such information may require a license from a third party under the patents or other intellectual property of the third party, or a license from TI under the patents or other intellectual property of TI.

TI REFERENCE DESIGNS ARE PROVIDED "AS IS". TI MAKES NO WARRANTIES OR REPRESENTATIONS WITH REGARD TO THE REFERENCE DESIGNS OR USE OF THE REFERENCE DESIGNS, EXPRESS, IMPLIED OR STATUTORY, INCLUDING ACCURACY OR COMPLETENESS. TI DISCLAIMS ANY WARRANTY OF TITLE AND ANY IMPLIED WARRANTIES OF MERCHANTABILITY, FITNESS FOR A PARTICULAR PURPOSE, QUIET ENJOYMENT, QUIET POSSESSION, AND NON-INFRINGEMENT OF ANY THIRD PARTY INTELLECTUAL PROPERTY RIGHTS WITH REGARD TO TI REFERENCE DESIGNS OR USE THEREOF. TI SHALL NOT BE LIABLE FOR AND SHALL NOT DEFEND OR INDEMNIFY BUYERS AGAINST ANY THIRD PARTY INFRINGEMENT CLAIM THAT RELATES TO OR IS BASED ON A COMBINATION OF COMPONENTS PROVIDED IN A TI REFERENCE DESIGN. IN NO EVENT SHALL TI BE LIABLE FOR ANY ACTUAL, SPECIAL, INCIDENTAL, CONSEQUENTIAL OR INDIRECT DAMAGES, HOWEVER CAUSED, ON ANY THEORY OF LIABILITY AND WHETHER OR NOT TI HAS BEEN ADVISED OF THE POSSIBILITY OF SUCH DAMAGES, ARISING IN ANY WAY OUT OF TI REFERENCE DESIGNS OR BUYER'S USE OF TI REFERENCE DESIGNS.

TI reserves the right to make corrections, enhancements, improvements and other changes to its semiconductor products and services per JESD46, latest issue, and to discontinue any product or service per JESD48, latest issue. Buyers should obtain the latest relevant information before placing orders and should verify that such information is current and complete. All semiconductor products are sold subject to TI's terms and conditions of sale supplied at the time of order acknowledgment.

TI warrants performance of its components to the specifications applicable at the time of sale, in accordance with the warranty in TI's terms and conditions of sale of semiconductor products. Testing and other quality control techniques for TI components are used to the extent TI deems necessary to support this warranty. Except where mandated by applicable law, testing of all parameters of each component is not necessarily performed.

TI assumes no liability for applications assistance or the design of Buyers' products. Buyers are responsible for their products and applications using TI components. To minimize the risks associated with Buyers' products and applications, Buyers should provide adequate design and operating safeguards.

Reproduction of significant portions of TI information in TI data books, data sheets or reference designs is permissible only if reproduction is without alteration and is accompanied by all associated warranties, conditions, limitations, and notices. TI is not responsible or liable for such altered documentation. Information of third parties may be subject to additional restrictions.

Buyer acknowledges and agrees that it is solely responsible for compliance with all legal, regulatory and safety-related requirements concerning its products, and any use of TI components in its applications, notwithstanding any applications-related information or support that may be provided by TI. Buyer represents and agrees that it has all the necessary expertise to create and implement safeguards that anticipate dangerous failures, monitor failures and their consequences, lessen the likelihood of dangerous failures and take appropriate remedial actions. Buyer will fully indemnify TI and its representatives against any damages arising out of the use of any TI components in Buyer's safety-critical applications.

In some cases, TI components may be promoted specifically to facilitate safety-related applications. With such components, TI's goal is to help enable customers to design and create their own end-product solutions that meet applicable functional safety standards and requirements. Nonetheless, such components are subject to these terms.

No TI components are authorized for use in FDA Class III (or similar life-critical medical equipment) unless authorized officers of the parties have executed an agreement specifically governing such use.

Only those TI components that TI has specifically designated as military grade or "enhanced plastic" are designed and intended for use in military/aerospace applications or environments. Buyer acknowledges and agrees that any military or aerospace use of TI components that have **not** been so designated is solely at Buyer's risk, and Buyer is solely responsible for compliance with all legal and regulatory requirements in connection with such use.

TI has specifically designated certain components as meeting ISO/TS16949 requirements, mainly for automotive use. In any case of use of non-designated products, TI will not be responsible for any failure to meet ISO/TS16949.